1 Introduction

The oscillation, or mixing, of the b-quark flavor is a well-known effect for B mesons. For example, in B_s meson system the mass eigenstates $|(B_s)_H\rangle$ and $|(B_s)_L\rangle$ with masses M_H and M_L are related to flavor eigenstates $|B_s\rangle = (\bar{b}s), |\bar{B}_s\rangle = (b\bar{s})$ as follows:

$$|(B_s)_H\rangle = \frac{1}{\sqrt{2}}(|B_s\rangle + |\bar{B}_s\rangle),$$

$$|(B_s)_L\rangle = \frac{1}{\sqrt{2}}(|B_s\rangle - |\bar{B}_s\rangle).$$

As a result, a B_s-meson born at time $t = 0$ as $|B_s\rangle$ may decay at time t as $|\bar{B}_s\rangle$ with probability

$$p(B_s \to \bar{B}_s) = \frac{e^{-t/\tau}}{2\tau}(1 + \cos\Delta m_s t).$$

Probability for $|B_s\rangle$ meson to keep its flavor at decay at time t is

$$p(B_s \to B_s) = \frac{e^{-t/\tau}}{2\tau}(1 - \cos\Delta m_s t).$$

Here τ is the B_s-meson lifetime. The parameter $\Delta m_s \equiv M_H - M_L$ is called "mixing frequency". It is important to know this parameter precisely, since it determines the behavior of B_s mesons system. Also, it is important to know the ratio of mixing frequencies $\Delta m_s/\Delta m_d$ for B_s and B_d systems, because it gives us constraint on CKM matrix elements. The Feynman diagrams describing B_s mixing are displayed in Figure 1. The transition is dominated by heavy t-quark, so that the CKM matrix elements V_{tb} and V_{ts} play an important role in the mixing phenomenon. Similar diagram for B_d includes V_{tb} and V_{td}, therefore the ratio $\Delta m_s/\Delta m_d$ allows us to constrain the ratio V_{ts}/V_{td}. More exactly,

$$\frac{\Delta m_s}{\Delta m_d} = \frac{m_{B_s}}{m_{B_d}} \cdot \xi^2 \cdot \frac{|V_{ts}|^2}{|V_{td}|^2},$$

where $\xi = -1.210^{+0.047}_{-0.035}$ (Reference [1]).

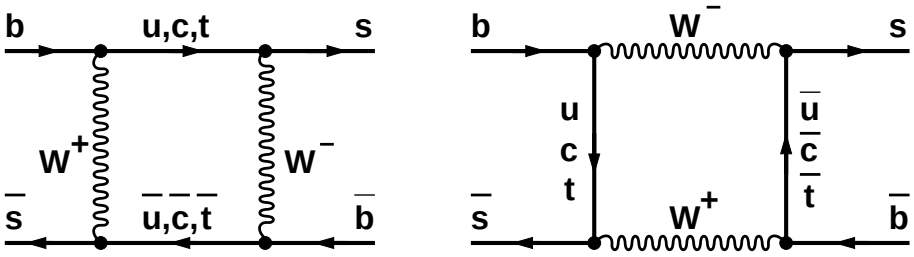

Figure 1: Feynman diagrams for B_s-mixing

In this analysis the tools for Δm_s measurement (tagging methods) are developed.

This note is organized as follows: in the next Section 2 we talk about B-flavor tagging in general. Section 3 describes the data and Monte Carlo samples used for the analysis. In Section 4 we discuss same-side tagging algorithms and their combination in Section 5. Section 6 is devoted to the measurement of the SST dilution by using double-tagged events in the data. Last comes the conclusion.

2 B-Flavor Tagging

To know if B-meson oscillated or not we need to to know (to "tag") its flavor at production and at decay. Let's consider semileptonic decays for simplicity. The flavor at decay can be easily obtained from the sign of trigger lepton (ℓ^+ corresponds to $\bar{b}$-quark, ℓ^- – to b-quark). The flavor at production is usually obtained with a special algorithm called "tagger". There are two main classes of such algorithms: Opposite-Side Taggers (OST) and Same-Side Taggers (SST). OST uses the fact that b-quarks are produced in b-$\bar{b}$ pairs. It determines the flavor of "the other" b-quark in pair which usually hadronizes and then fragments into a jet on "the other" (opposite) side of the event (Figure 2). The average charge of the tracks in this jet gives a charge, and thus a flavor, of "the other" b-quark, from which we infer the initial flavor of the b-quark inside the B-meson. This method is called "jet-charge" tagger. If a soft lepton is found among the tracks in the jet on "the other" side, then the flavor of "the other" b-quark can be obtained from the charge of this lepton only ("soft-lepton" tagger).

SST uses the tracks on the same side of the event as the B-meson. The principle of its work is clear from the Figure 3. The b-quark "picks up" a u, d or s quark from a q-$\bar{q}$ pair and the remaining quark in the pair forms a meson (or even hyperon) with some other quark(s). If this meson is charged we can reconstruct its track and from its charge infer the information about the b-quark flavor at production. B meson born as B_d is likely to have a π^+ nearby (π^- for $\overline{B}_d$). Similarly, B meson born as B_s is likely to have a K^+ nearby (K^- for $\overline{B}_s$).

There are different methods of finding the particle which was born together with B meson (different same-side taggers). All of them can be divided into three groups:

- Taggers using one track, selected accroding to some kinemtic requirements
- Taggers reconstructing resonances, such as K^{*0} or Λ, decaying into two tracks
- Taggers using all the tracks in the vicinity of the B-meson

Particular implementation of these taggers will be considered in Section 4.

For each event taggers conclude if the B-meson did not oscillate (*i.e.* the charge of the tag is the same as lepton charge, "Right-Sign"), or if it did (*i.e.* the charge of the tag is opposite to the lepton charge, "Wrong-Sign"), or if no tag was found ("No-Tag"). The main tagger characteristics are the following:

- tagging efficiency $\varepsilon = \frac{N_{RS}+N_{WS}}{N_{RS}+N_{WS}+N_{NT}}$
- *raw* dilution D_{raw} or asymmetry $A = \frac{N_{RS}-N_{WS}}{N_{RS}+N_{WS}}$
- (*true*) dilution $D = 1 - 2p$, where p is a mistag rate, which can be obtained from MC if true B-flavor at production is known
- tagging power εD^2 or $\varepsilon D^2_{\text{raw}}$

It can be shown that the error on Δm_s is inversely proportional to $\sqrt{\varepsilon D^2}$, so that it is

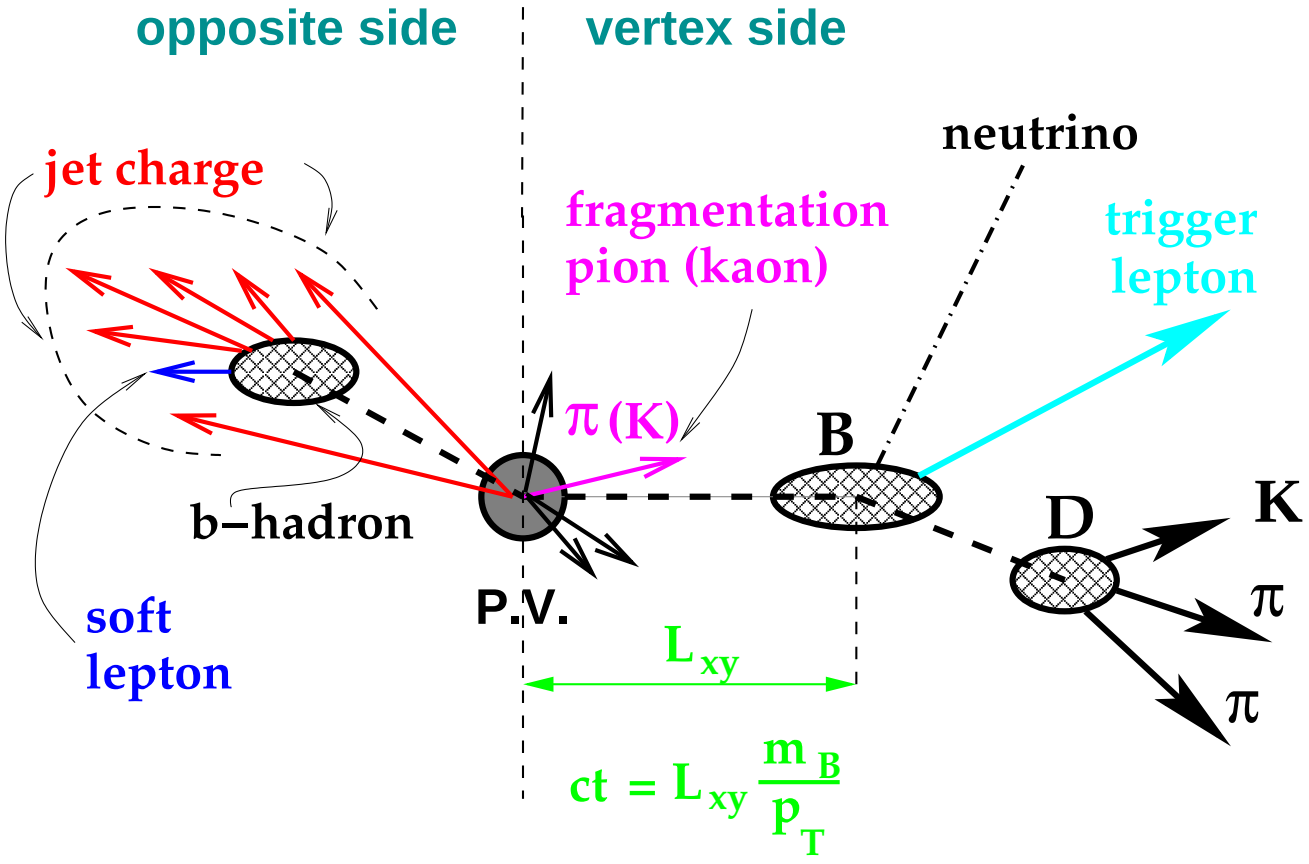

Figure 2: The sketch of the event with a B-meson

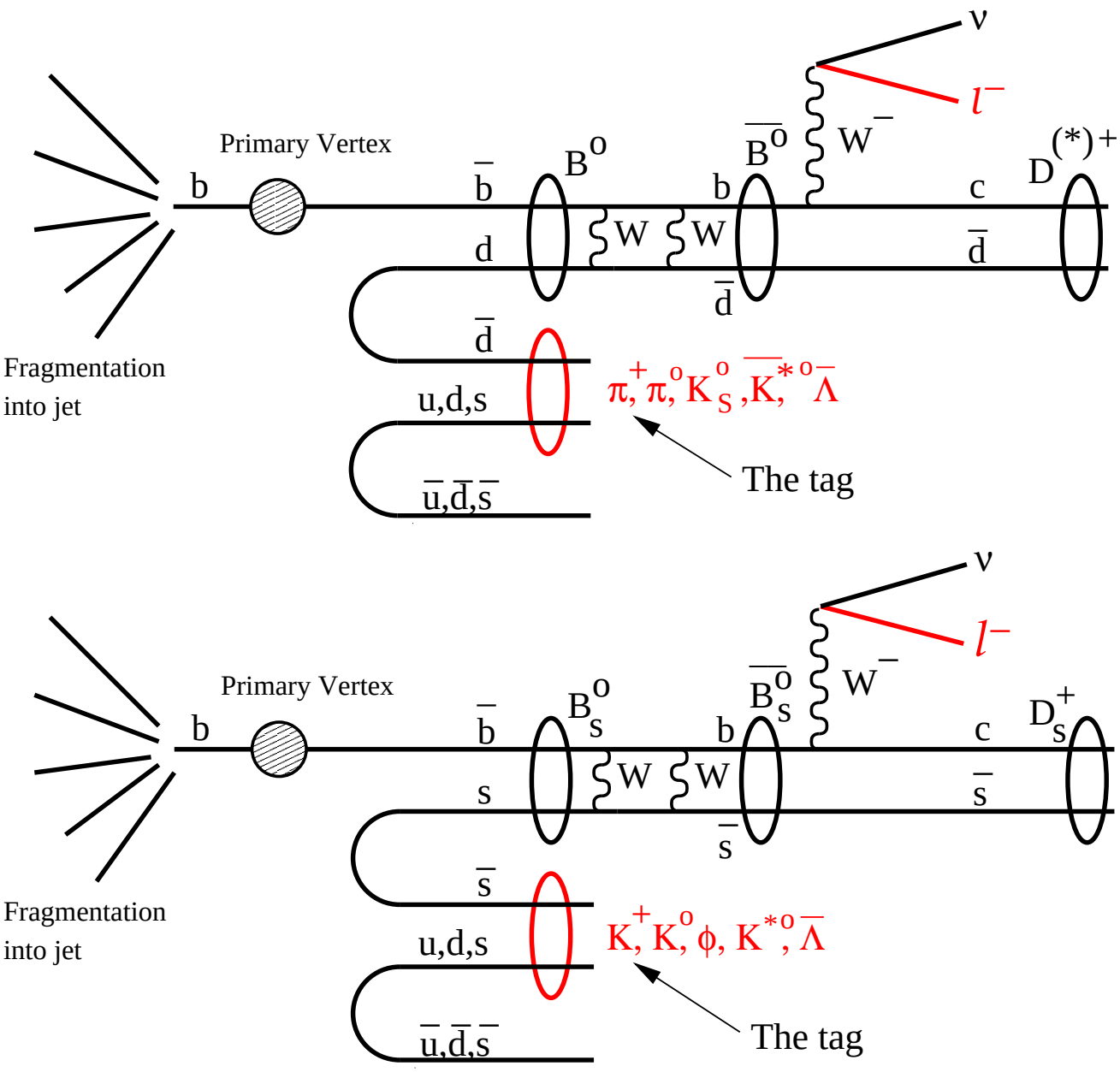

Figure 3: The scheme of SST

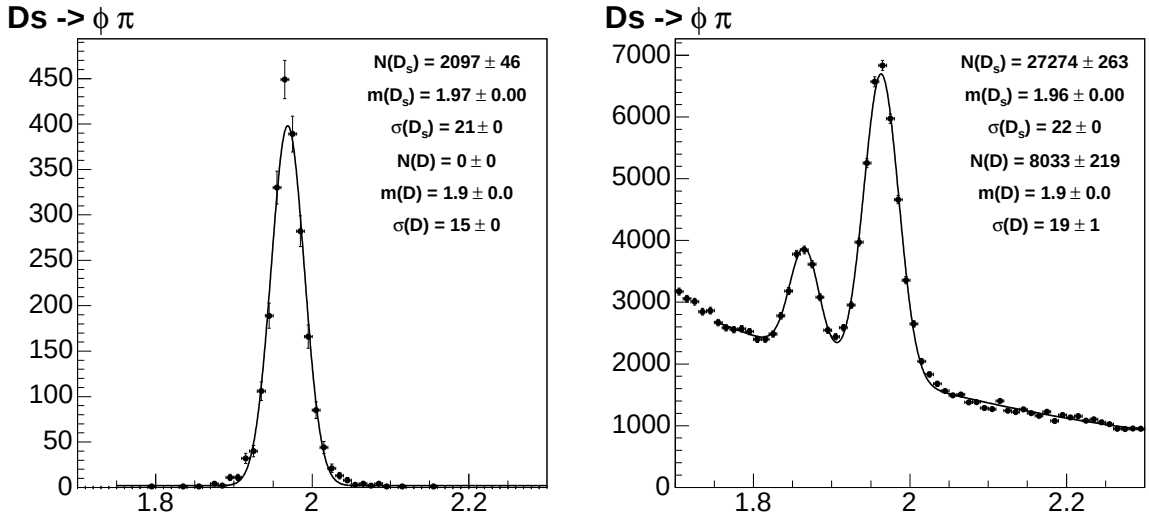

Figure 4: The D_s mass histograms in Monte Carlo and in the data

important to use taggers with high tagging power in the analysis.

3 Monte Carlo and Data Samples Used in the Analysis

The following Monte Carlo samples are used to study SST:

- $B_s \to \mu D_s, D_s \to \phi\pi, (x_s = 25)$, request 15425 (p14)
- $B_s \to \mu D_s, D_s \to \phi\pi, (x_s = 25)$, requests 29892, 29893 (p17)

To make sure that Monte Carlo matches the data we compare various distributions in Monte Carlo and in the data selected in `/prj_root/1008/ckm_write/bgv/evt/muphipi-std/` (1 fb^{-1}).

The mass histogram of D_s in the Monte Carlo and the data is shown in Figure 4. The sideband-subtracted data distributions are to be compared to the Monte Carlo ones. The signal and sideband regions are chosen to be (1.91,2.01) and (1.75,1.80) $\bigcup$ (2.12,2.17) GeV/c^2.

The Monte Carlo–data match of the important for SST distributions (see details in Section 4.1) is shown in Figure 5 for p17 Monte Carlo and in Figure 6 for p14 one. Magenta crosses represent the data, green histograms – Monte Carlo. We see that p17 MC matches the data much better than p14, though some discrepancies still occur at low p_t^{rel} region. For the analysis we only use p17 Monte Carlo. But for the comparison puposes we give the dilutions and ϵD^2's for p14 Monte Carlo as well – see Appendix A.

4 SST Algorithms and Their Performance in Monte Carlo

Since in Monte Carlo we know the true b-quark flavor at production, we can determine the number of the events with correct charge of the tag ("Right-Tag") and the opposite charge of the

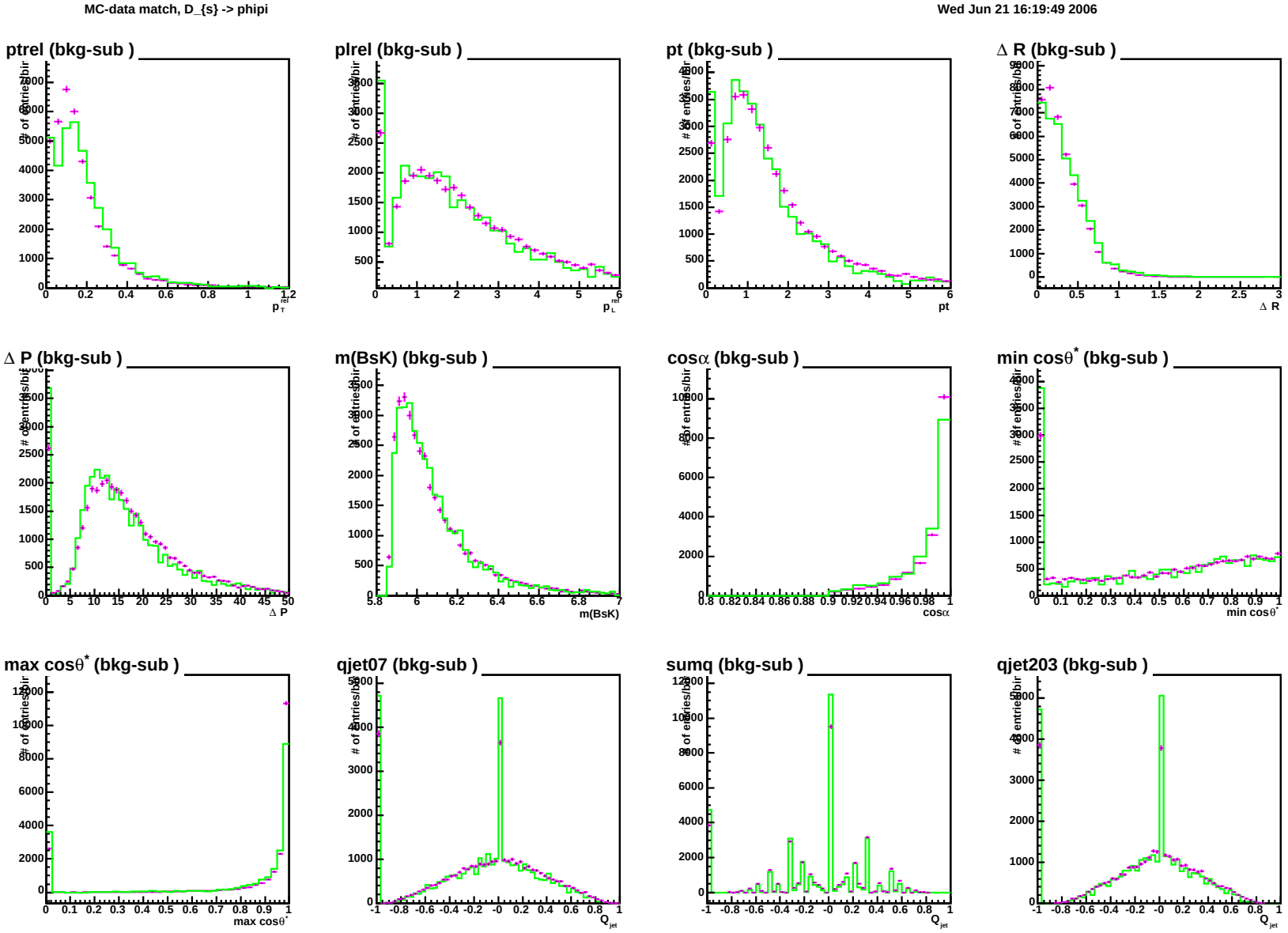

Figure 5: The p17 Monte Carlo–data match for various quantities (see Sections 4.1, 4.3)

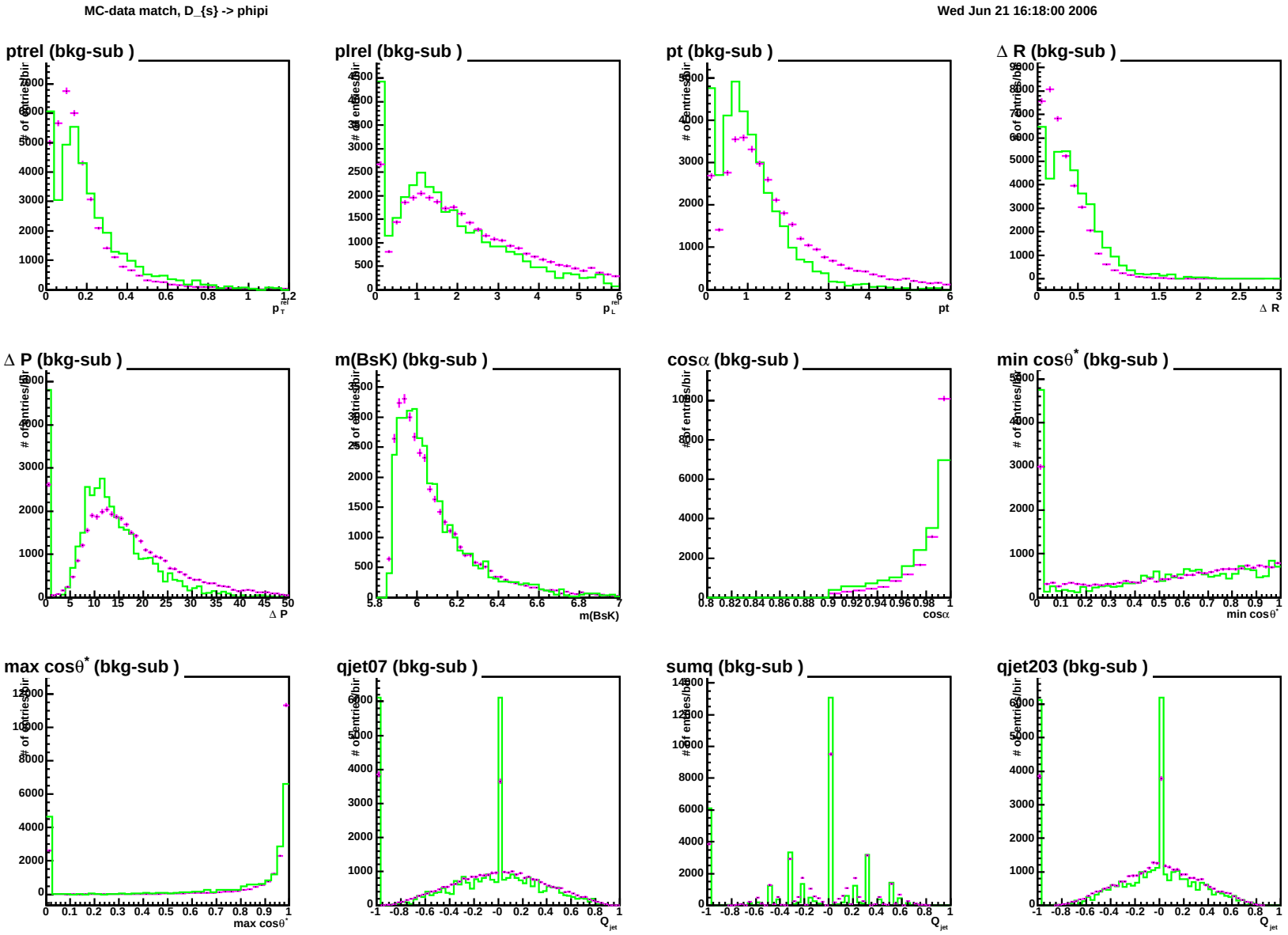

Figure 6: The p14 Monte Carlo–data match for various quantities (see Sections 4.1, 4.3)

tag ("Wrong-Tag"). Thus we obtain the mistag rate $p = \frac{N_{WT}}{N_{RT}+N_{WT}}$, and, therefore, *true* dilution $D = 1 - 2p$ for the taggers above. Also, we obtain the number of the events where tag was not found ("No-Tag") and the tagging efficiency $\epsilon = \frac{N_{RT}+N_{WT}}{N_{RT}+N_{WT}+N_{NT}}$.

To tag the flavor of the B-meson at the production stage we look at the tracks in cone $\cos\alpha < 0.8$ around 3-dimensional momentum of B-meson, $\vec{p}(B_s)$. The tracks are supposed to have at least 2 SMT axial hits and at least 3 CFT axial hits.

4.1 SST Algorithms Using One Track

The following algorithms were used to select one-track tag (see left part of Figure 7):

- Min. $p_t^{\rm rel}$
- Max. $p_L^{\rm rel}$
- Max. p_t
- Min. $|\Delta\vec{P}| \equiv |\vec{p}(B_s) - \vec{p}(K)|$
- Min. ΔR
- Max. $\cos\alpha$
- Min. $\cos\theta^*$
- Max. $\cos\theta^*$
- Min. $m(B_sK)$

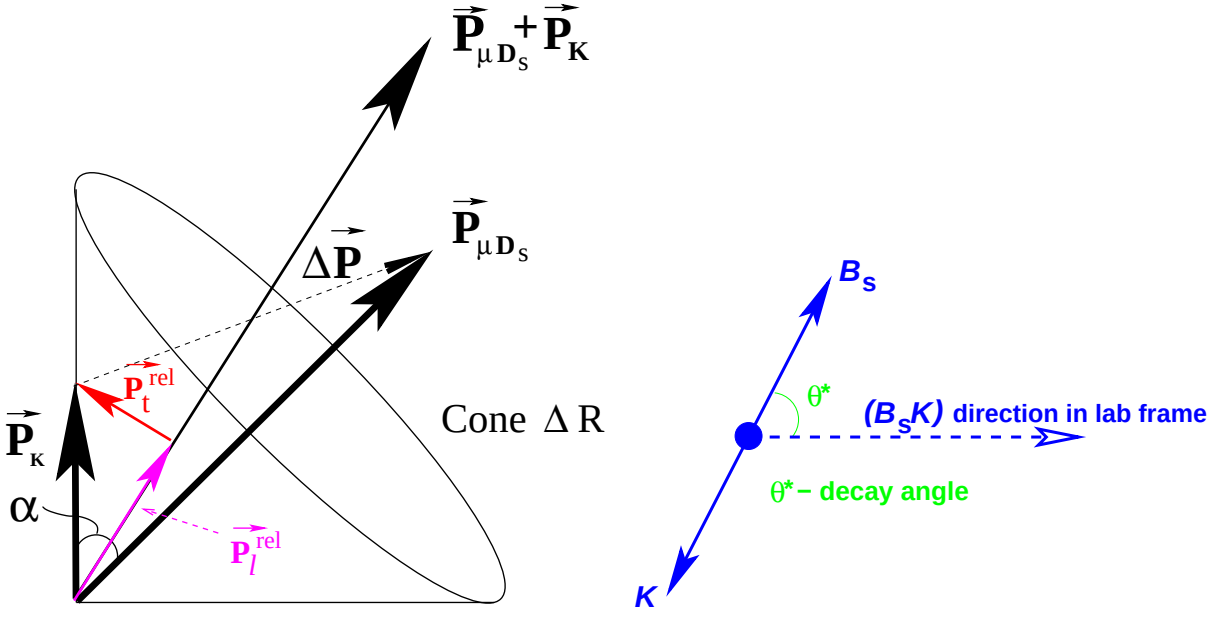

Figure 7: **Left:** One-track SST selection; **Right:** θ^* – decay angle of B_sK-system.

Here $p_t^{\rm rel}$ and $p_L^{\rm rel}$ are $\perp$ and $||$ components of SST candidate's momentum $\vec{p}(K)$ w.r.t $\vec{p}(B_sK)$. The $\Delta R \equiv \sqrt{\Delta\phi^2 + \Delta\eta^2}$ and angle α are taken between $\vec{p}(B_s)$ and $\vec{p}(K)$. The θ^* – decay angle of B_sK-system, *i.e.* angle between directions of $\vec{p}(B_sK)$ and $\vec{p}(B_s)$ in reference frame of B_sK system, as shown in the right part of Figure 7.

The *true* dilutions and ϵD^2's for these taggers are obtained for p17 Monte Carlo and are given in Table 1 and the ϵD^2's are graphically compared in Figure 8. The dilutions and ϵD^2's for p14 Monte Carlo are given in Appendix A for comparison purposes.

Tagger	N_{RT}	N_{WT}	N_{NT}	$\varepsilon, \%$	D, %	$\varepsilon \mathrm{D}^2, \%$
Min. p_t^{rel}	1043 ± 32	941 ± 31	217 ± 15	90.1 ± 0.6	5.1 ± 2.2	0.238 ± 0.198
Max. p_L^{rel}	1020 ± 32	964 ± 31	217 ± 15	90.1 ± 0.6	2.8 ± 2.2	0.072 ± 0.111
Max. p_t	1029 ± 32	955 ± 31	217 ± 15	90.1 ± 0.6	3.7 ± 2.2	0.125 ± 0.146
Min. $\lvert\Delta\vec{P}\rvert$	1022 ± 32	962 ± 31	217 ± 15	90.1 ± 0.6	3.0 ± 2.2	0.082 ± 0.119
Min. ΔR	1037 ± 32	947 ± 31	217 ± 15	90.1 ± 0.6	4.5 ± 2.2	0.185 ± 0.176
Max. $\cos\alpha$	1024 ± 32	960 ± 31	217 ± 15	90.1 ± 0.6	3.2 ± 2.2	0.094 ± 0.127
Min. $\cos\theta^*$	1022 ± 32	962 ± 31	217 ± 15	90.1 ± 0.6	3.0 ± 2.2	0.082 ± 0.119
Max. $\cos\theta^*$	1041 ± 32	943 ± 31	217 ± 15	90.1 ± 0.6	4.9 ± 2.2	0.220 ± 0.191
Min. $m(B_sK)$	1007 ± 32	977 ± 31	217 ± 15	90.1 ± 0.6	1.5 ± 2.2	0.021 ± 0.060

Table 1: Comparison of different one-track taggers

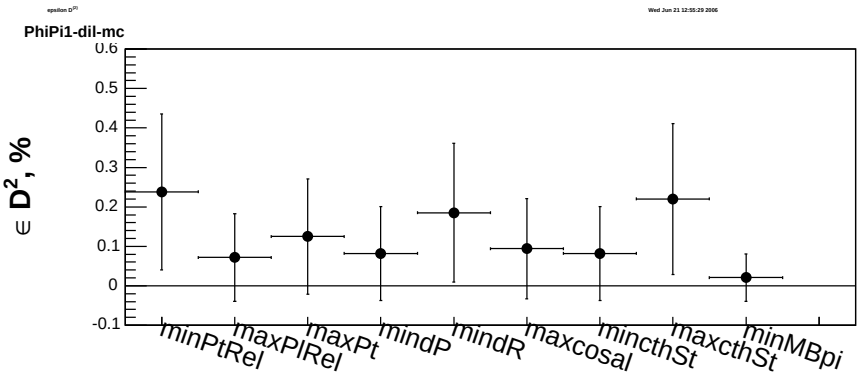

Figure 8: Comparison between $\varepsilon \mathrm{D}^2$'s for one-track taggers

Of course, all the one-track taggers are highly correlated to each other. So we will choose one of them which gives the best result (has largest $\varepsilon \mathrm{D}^2$) and will be using only it. From Figure 8 one can see that "Min. p_t^{rel}" is the best tagger.

4.2 Using Kaons Coming from K^{*0} and Pions From Λ:

Another group of taggers is based on reconstruction of two-track resonance in the vicinity of B-meson: $K^{*0} \to K\pi$ and $\Lambda \to p\pi$. The sign of kaon (pion for Λ) helps infer the b-quark flavor at production. The K^{*0} is reconstructed out of two oppositely charged tracks assigned with masses of kaon and pion and with invariant mass being $0.842\ \mathrm{GeV}/c^2 < m(K^{*0} \to K\pi) < 0.942\ \mathrm{GeV}/c^2$. The auto-reflection (same track combination with opposite mass assignment) is required to be outside of this mass window so that we could know for sure which track is kaon and which is pion. Both these tracks are required to be within cone $\cos\alpha > 0.8$ around $\vec{p}(B_s)$ and to have at least 2 axial hits in SMT and 3 axial hits in CFT. The B_s daughters are excluded. The mass distributions of so found K^{*0} for MC and data are given in Figure 9. They are sideband-subtracted with respect to D_s mass.

Another implementation of the same tagger ("optimized K^{*0}") is created with a few additional cuts applied to the reconstructed K^{*0}'s:

- $\Delta R \equiv \sqrt{\Delta\phi^2 + \Delta\eta^2} < 0.3$ between the tracks
- Both tracks' impact parameter $|d_0/\sigma_{d_0}| > 3$
- Vertex $\chi^2 < 20$
- Isolation $\frac{|\vec{p}(K^{*0})|}{|\vec{p}(K^{*0})| + \sum\limits_{tracks\ \ with\ \ \Delta R<0.5} |\vec{p}|} > 0.4$
- Cosine of the angle between the momentum of the positive track and the direction of the K^{*0} in the rest frame of K^{*0}, $|\cos\theta^*| < 0.4$

The mass distributions of K^{*0} for MC and data after these cuts (sideband-subtracted with respect to D_s mass) are demonstrated in Figure 10.

The reconstruction of $\Lambda \to p\pi$ is also performed only with tracks within cone $\cos\alpha > 0.8$ around $\vec{p}(B)$ and having 2+ axial SMT hits and 3+ axial CFT hits. The B daughters are again excluded. The standard reconstruction algorithm from `AA::v0Finder` from `bana` package is employed. The D_s-sideband-subtracted mass histogram is shown in Figure 11.

The comparison of the taggers is given in Table 2 and, in graphical form, in Figure 12. The performance of the "K^{*0}" is better than the "Optimized K^{*0}", so we are choosing the former one. Since tagger "Lambda" is uncorrelated with "K^{*0}" by construction, we will be using both of them.

Tagger	N_{RT}	N_{WT}	N_{NT}	$\varepsilon, \%$	D, %	$\varepsilon \mathrm{D}^2, \%$
$K^{*0} \to K\pi$	349 ± 19	329 ± 18	1523 ± 39	30.8 ± 1.0	2.9 ± 3.8	0.027 ± 0.068
$K^{*0} \to K\pi$(opt)	46 ± 7	48 ± 7	2107 ± 46	4.3 ± 0.4	-2.1 ± 10.3	0.002 ± 0.019
Λ	6 ± 2	8 ± 3	2187 ± 47	0.6 ± 0.2	-14.3 ± 26.5	0.013 ± 0.052

Table 2: Comparison of different two-track taggers

4.3 Using Weighted-Average Charge

The last group of same-side taggers is based on the weighted charge of **all** the tracks within cone $\cos\alpha > 0.8$, having 2+ axial SMT and 3+ axial CFT hits with B daughters excluded. We utilize

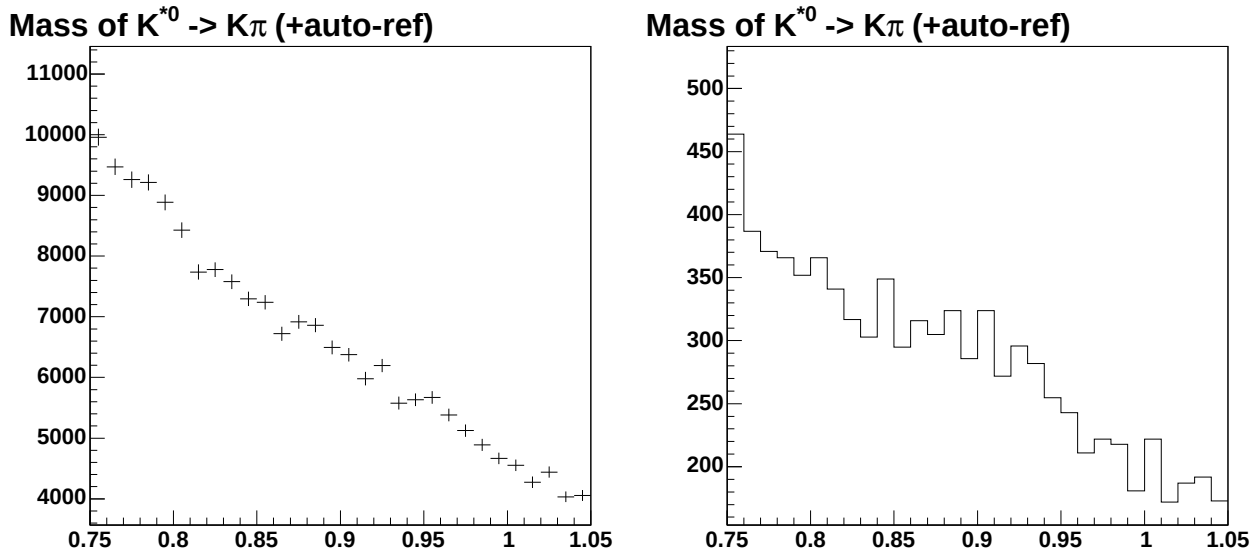

Figure 9: K^{*0} mass: data (left) and MC (right)

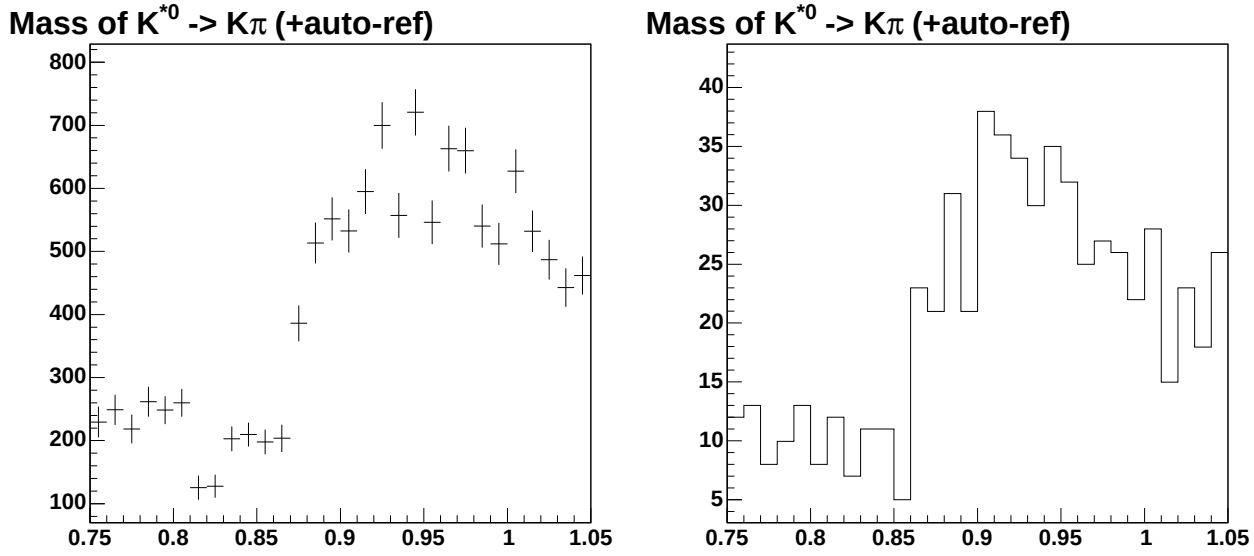

Figure 10: "Optimized" K^{*0} mass: data (left) and MC (right)

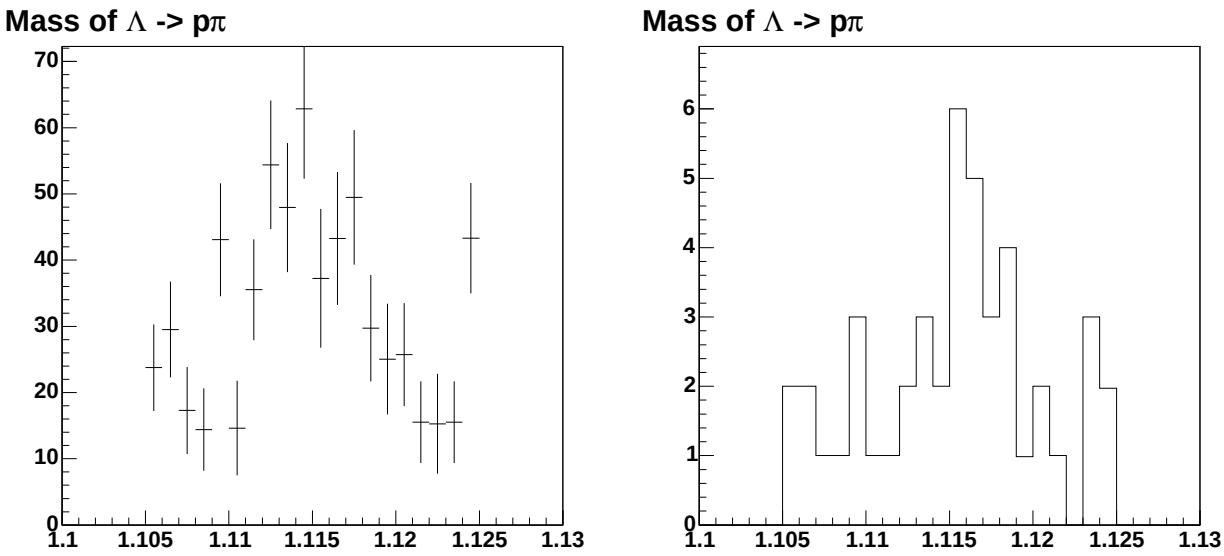

Figure 11: Λ mass: data (left) and MC (right)

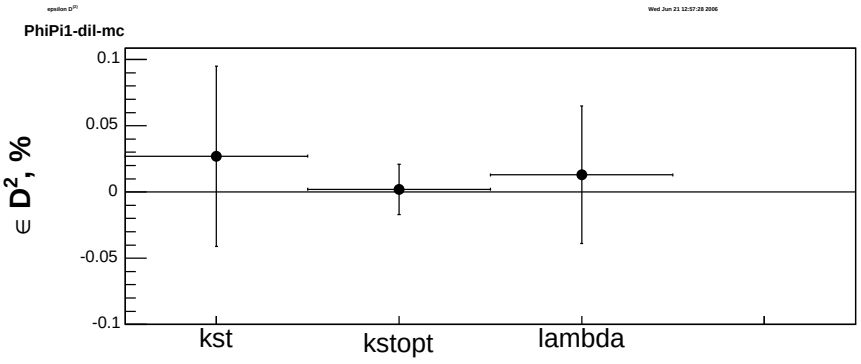

Figure 12: Comparison between εD^2's for two-track taggers

Tagger	N_{RT}	N_{WT}	N_{NT}	$\varepsilon, \%$	D, %	$\varepsilon \mathrm{D}^2, \%$
Aver. Q	760 ± 28	625 ± 25	816 ± 29	62.9 ± 1.0	9.7 ± 2.7	0.598 ± 0.304
$Q_{jet}(p_t, \kappa = 0.1)$	711 ± 27	593 ± 24	897 ± 30	59.2 ± 1.0	9.0 ± 2.8	0.485 ± 0.276
$Q_{jet}(p_t, \kappa = 0.2)$	706 ± 27	595 ± 24	900 ± 30	59.1 ± 1.0	8.5 ± 2.8	0.430 ± 0.261
$Q_{jet}(p_t, \kappa = 0.3)$	712 ± 27	597 ± 24	892 ± 30	59.5 ± 1.0	8.8 ± 2.8	0.459 ± 0.269
$Q_{jet}(p_t, \kappa = 0.4)$	724 ± 27	608 ± 25	869 ± 29	60.5 ± 1.0	8.7 ± 2.7	0.459 ± 0.269
$Q_{jet}(p_t, \kappa = 0.5)$	737 ± 27	622 ± 25	842 ± 29	61.7 ± 1.0	8.5 ± 2.7	0.442 ± 0.264
$Q_{jet}(p_t, \kappa = 0.6)$	758 ± 28	623 ± 25	820 ± 29	62.7 ± 1.0	9.8 ± 2.7	0.600 ± 0.304
$Q_{jet}(p_t, \kappa = 0.7)$	774 ± 28	632 ± 25	795 ± 28	63.9 ± 1.0	10.1 ± 2.7	0.652 ± 0.316
$Q_{jet}(p_t, \kappa = 0.8)$	782 ± 28	647 ± 25	772 ± 28	64.9 ± 1.0	9.4 ± 2.6	0.579 ± 0.299
$Q_{jet}(p_t, \kappa = 0.9)$	801 ± 28	661 ± 26	739 ± 27	66.4 ± 1.0	9.6 ± 2.6	0.609 ± 0.306
$Q_{jet}(p_t, \kappa = 1.0)$	812 ± 28	682 ± 26	707 ± 27	67.9 ± 1.0	8.7 ± 2.6	0.514 ± 0.283

Table 3: Comparison of different charge-average taggers

Tagger	N_{RT}	N_{WT}	N_{NT}	$\varepsilon, \%$	D, %	$\varepsilon \mathrm{D}^2, \%$
Aver. Q	760 ± 28	625 ± 25	816 ± 29	62.9 ± 1.0	9.7 ± 2.7	0.598 ± 0.304
$Q_{jet}(p_t^{rel}, \kappa = 0.1)$	700 ± 26	596 ± 24	905 ± 30	58.9 ± 1.0	8.0 ± 2.8	0.379 ± 0.246
$Q_{jet}(p_t^{rel}, \kappa = 0.2)$	694 ± 26	601 ± 25	906 ± 30	58.8 ± 1.0	7.2 ± 2.8	0.303 ± 0.221
$Q_{jet}(p_t^{rel}, \kappa = 0.3)$	711 ± 27	604 ± 25	886 ± 30	59.7 ± 1.0	8.1 ± 2.7	0.396 ± 0.251
$Q_{jet}(p_t^{rel}, \kappa = 0.4)$	730 ± 27	627 ± 25	844 ± 29	61.7 ± 1.0	7.6 ± 2.7	0.355 ± 0.239
$Q_{jet}(p_t^{rel}, \kappa = 0.5)$	750 ± 27	653 ± 26	798 ± 28	63.7 ± 1.0	6.9 ± 2.7	0.305 ± 0.222
$Q_{jet}(p_t^{rel}, \kappa = 0.6)$	766 ± 28	675 ± 26	760 ± 28	65.5 ± 1.0	6.3 ± 2.6	0.261 ± 0.206
$Q_{jet}(p_t^{rel}, \kappa = 0.7)$	779 ± 28	697 ± 26	725 ± 27	67.1 ± 1.0	5.6 ± 2.6	0.207 ± 0.185
$Q_{jet}(p_t^{rel}, \kappa = 0.8)$	803 ± 28	713 ± 27	685 ± 26	68.9 ± 1.0	5.9 ± 2.6	0.243 ± 0.200
$Q_{jet}(p_t^{rel}, \kappa = 0.9)$	821 ± 29	728 ± 27	652 ± 26	70.4 ± 1.0	6.0 ± 2.5	0.254 ± 0.204
$Q_{jet}(p_t^{rel}, \kappa = 1.0)$	839 ± 29	743 ± 27	619 ± 25	71.9 ± 1.0	6.1 ± 2.5	0.265 ± 0.208

Table 4: Comparison of different charge-average taggers

three different methods of averaging:

- $Q_{jet}(p_t, \kappa) = \frac{\sum q \cdot p_t^{\kappa}}{\sum p_t^{\kappa}}$
- $Q_{jet}(p_t^{rel}, \kappa) = \frac{\sum q \cdot (p_t^{rel})^{\kappa}}{\sum (p_t^{rel})^{\kappa}}$
- $Q_{jet}(p_L^{rel}, \kappa) = \frac{\sum q \cdot (p_L^{rel})^{\kappa}}{\sum (p_L^{rel})^{\kappa}}$

Here p_t^{rel} and p_L^{rel} are $\perp$ and $||$ components of SST candidate's momentum $\vec{p}(K)$ w.r.t $\vec{p}(B_s)$. p_t is a tranverse component of the SST candidate's momentum w.r.t. the beamline. The parameter κ increases the sensitivity to a particular region of p_t spectrum and must be optimized. We impose the cut $|Q_{jet}| > 0.2$. The results for different many-track taggers are given in Tables 3,4,5 and in graphical form in Figure 13. The best tagger is "$Q_{jet}(p_t, \kappa = 0.7)$".

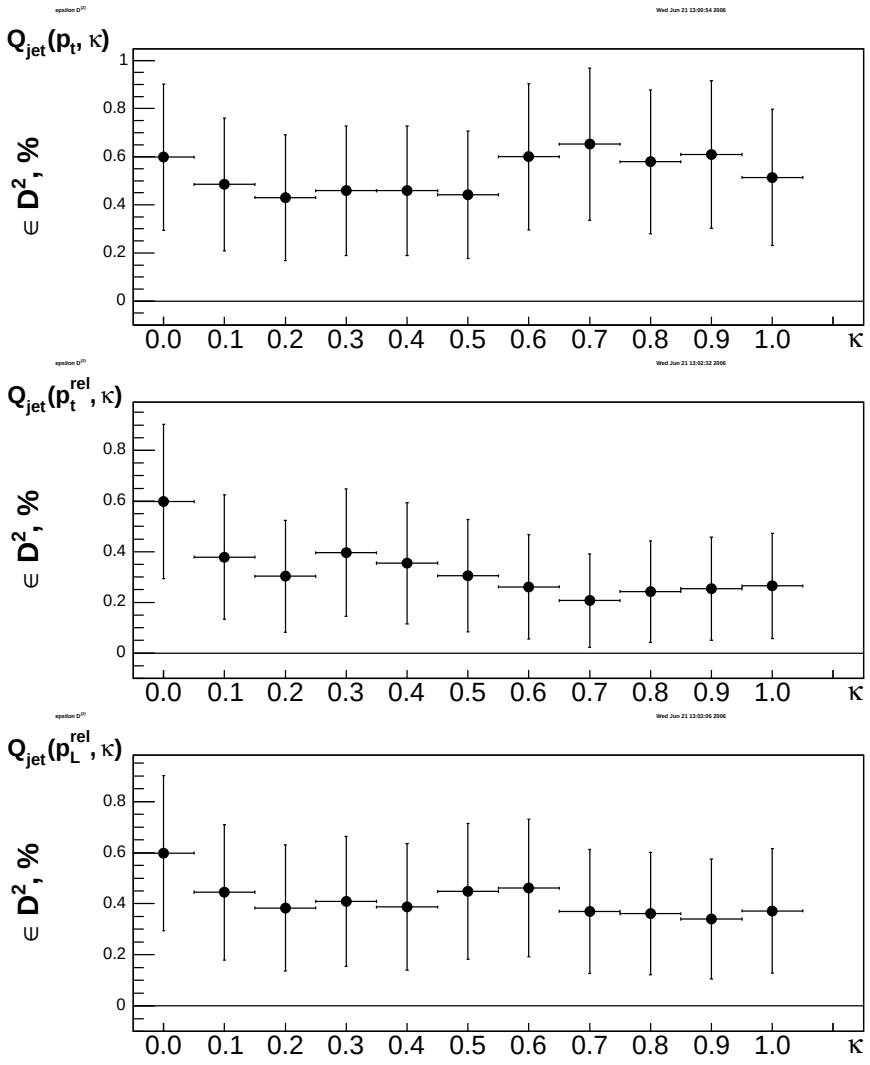

Figure 13: Comparison between εD^2's for charge-average taggers

Tagger	N_{RT}	N_{WT}	N_{NT}	$\varepsilon, \%$	D, %	$\varepsilon \mathrm{D}^2, \%$
Aver. Q	760 ± 28	625 ± 25	816 ± 29	62.9 ± 1.0	9.7 ± 2.7	0.598 ± 0.304
$Q_{jet}(p_L^{rel}, \kappa = 0.1)$	709 ± 27	596 ± 24	896 ± 30	59.3 ± 1.0	8.7 ± 2.8	0.445 ± 0.265
$Q_{jet}(p_L^{rel}, \kappa = 0.2)$	707 ± 27	602 ± 25	892 ± 30	59.5 ± 1.0	8.0 ± 2.8	0.383 ± 0.247
$Q_{jet}(p_L^{rel}, \kappa = 0.3)$	715 ± 27	606 ± 25	880 ± 30	60.0 ± 1.0	8.3 ± 2.7	0.409 ± 0.255
$Q_{jet}(p_L^{rel}, \kappa = 0.4)$	725 ± 27	618 ± 25	858 ± 29	61.0 ± 1.0	8.0 ± 2.7	0.387 ± 0.248
$Q_{jet}(p_L^{rel}, \kappa = 0.5)$	740 ± 27	624 ± 25	837 ± 29	62.0 ± 1.0	8.5 ± 2.7	0.448 ± 0.266
$Q_{jet}(p_L^{rel}, \kappa = 0.6)$	757 ± 28	638 ± 25	806 ± 28	63.4 ± 1.0	8.5 ± 2.7	0.461 ± 0.269
$Q_{jet}(p_L^{rel}, \kappa = 0.7)$	757 ± 28	650 ± 25	794 ± 28	63.9 ± 1.0	7.6 ± 2.7	0.370 ± 0.243
$Q_{jet}(p_L^{rel}, \kappa = 0.8)$	774 ± 28	667 ± 26	760 ± 28	65.5 ± 1.0	7.4 ± 2.6	0.361 ± 0.240
$Q_{jet}(p_L^{rel}, \kappa = 0.9)$	789 ± 28	684 ± 26	728 ± 27	66.9 ± 1.0	7.1 ± 2.6	0.340 ± 0.234
$Q_{jet}(p_L^{rel}, \kappa = 1.0)$	807 ± 28	696 ± 26	698 ± 26	68.3 ± 1.0	7.4 ± 2.6	0.372 ± 0.244

Table 5: Comparison of different charge-average taggers

5 SST Combination Technique

The combination of SSTs is performed according to the algorithm developed for OSTs in Reference [2]. First, we look for any discriminating variables x_i which have different probability density functions $f_i^b(x_i)$ and $f_i^{\bar{b}}(x_i)$ for b and $\bar{b}$ quarks. These functions are taken from Monte Carlo (as opposed to OST case, where they are taken from data sample $B_d \to \mu D^{*0}$). Second, we form a ratio $y_i(x_i) = \frac{f_i^b(x_i)}{f_i^{\bar{b}}(x_i)}$. The case $y_i(x_i) > 1$ corresponds to b-quark, the opposite case $y_i(x_i) < 1$ – to $\bar{b}$-quark. Third, we define a variable $y(\vec{x}) = \prod_{i=1}^{n} y_i(x_i)$ which accumulates information from all the discriminating variables. Now, for each event, $y(\vec{x}) > 1$ corresponds to b-quark, the opposite case $y(\vec{x}) < 1$ – to $\bar{b}$-quark. For combination we use four least correlated between themselves taggers from different groups: "Min. p_t^{rel}", "K^{*0}", "Lambda" and "$Q_{jet}(p_t, \kappa = 0.7)$". The variables x_i are: $x_1 = q \cdot p_t^{rel}$, $x_2 = q \cdot (m(K^{*0}) - 0.842)/(0.942 - 0.842)$, $x_3 = q \cdot (m(\Lambda) - 1.105)/(1.125 - 1.105)$, and $x_4 = Q_{jet}$, where q is the charge of the tag.

For each event the B-meson production flavor is obtained from the Monte Carlo truth information and then corresponding histogram is filled to produce p.d.f. $f_i^b(x_i)$ or $f_i^{\bar{b}}(x_i)$. The probability density functions for all four variables x_1, x_2, x_3, x_4 are shown in Figure 14.

We construct the variable y as the product of the ratios of p.d.f.'s above and then compute the combined dilution $d = \frac{1-y}{1+y}$ for each event. The distribution of this quantity d should give us the largest discrimination between b and $\bar{b}$ quarks. This distribution is shown in Figure 15.

6 Tagger Combination with Double-Tagged Events:

Using both SST and OST on the same data sample allows one to measure the product of their dilutions $D_{OST} \cdot D_{SST}$ (see Appendix B). By using D_{OST} measured earlier Reference [3], we can obtain the D_{SST} purely from the data (Equation 3). Then we can compute the tagging power ϵD^2 of

"Min. p_t^{rel}"

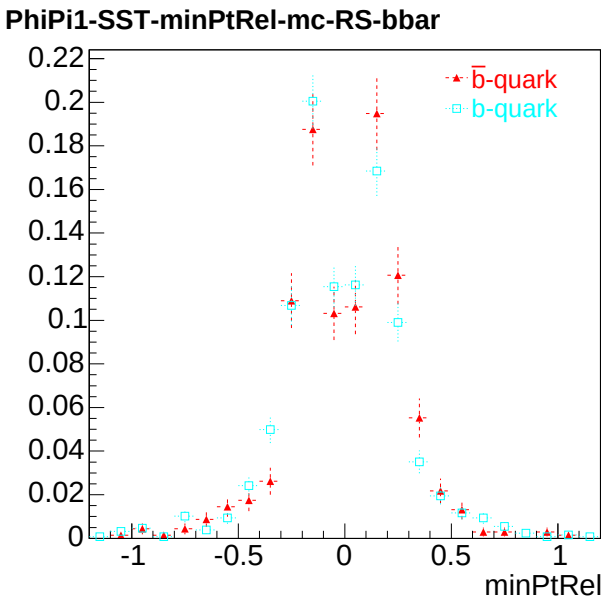

"K^{*0}"

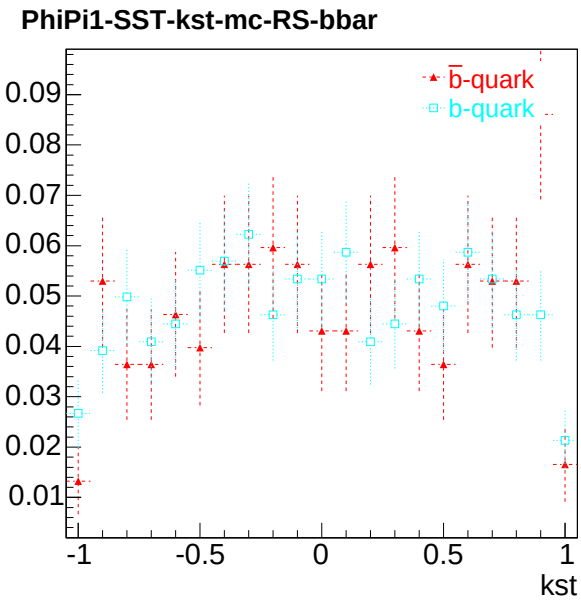

"Lambda"

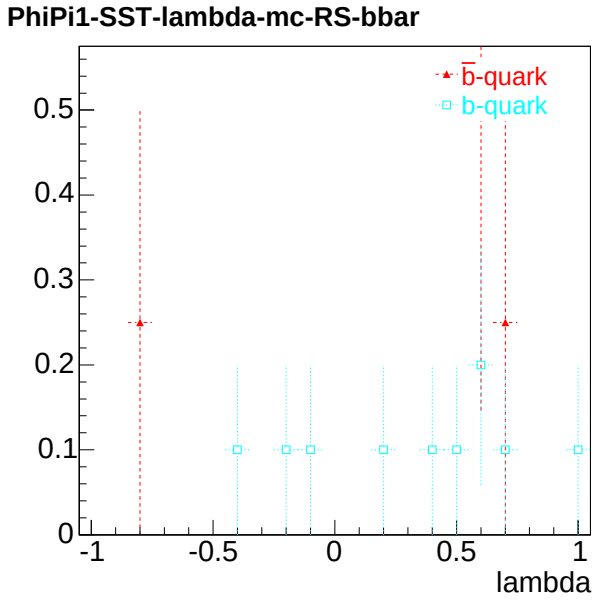

"$Q_{jet}(p_t, \kappa = 0.7)$"

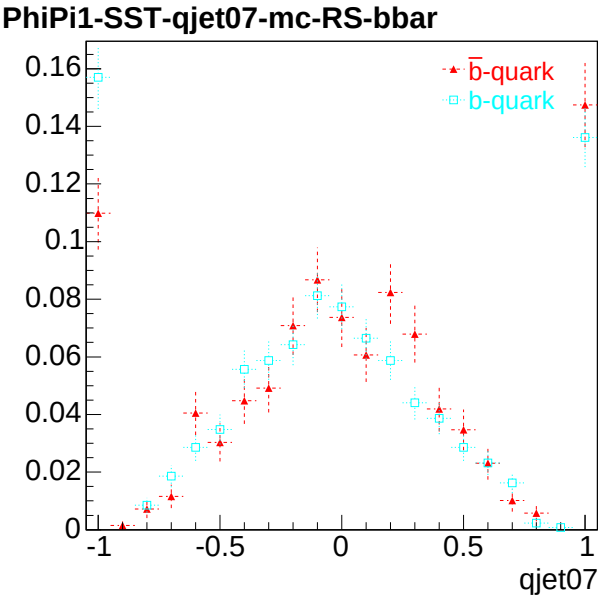

Figure 14: The probability density functions for "Min. p_t^{rel}", "optimized K^{*0}", "Lambda" and "$Q_{jet}(p_t, \kappa = 0.7)$". Red full triangles - p.d.f. for $\bar{b}$-quark, cyan open squares - p.d.f. for b-quark.

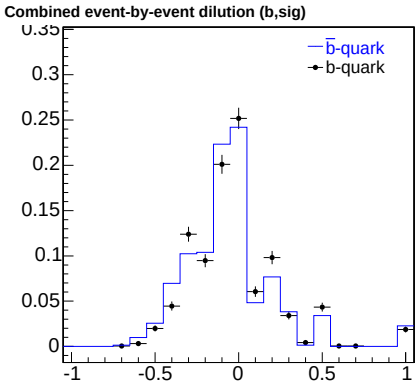

Figure 15: Distribution of combined dilution d

the combination of SST and OST (Equation 4). We do so for each considered SST algorithm and for final combined SST algorithm for the data in `/prj_root/1008/ckm_write/bgv/evt/muphipi-std/` (1 fb^{-1}). The results are given in Table 6.

7 Conclusion

In this note a technique developed for combination of opposite-side taggers (Reference [2]) is implemented for same-side taggers. A few same-side taggers are chosen ("Min. p_t^{rel}", "K^{*0}", "Lambda" and "$Q_{jet}(p_t, \kappa = 0.7)$") to be combined together. Also, double-tagged events are used to apply both "Comb. SST" and OST to the data. This allows to measure SST dilution from data only, by using earlier measured OST dilution (Reference [3])). The total ϵD^2's for both SST and OST are given in Table 6.

References

[1] hep/lat-0510113

[2] G. Borissov *et al.*, *Combined Opposite-side Flavor Tagging*, **D0 Note 4875**, (July 8, 2005).

[3] G. Borissov *et al.*, *B_d mixing measurement using Opposite-side Flavor Tagging*, **D0 Note 4991**, (Feb 17, 2006).

[4] P. Sphicas, *Combining Flavor-Taggers*, **CDF Note 3425**, (Dec 9, 1995).

	N_1	N_2	N_{NT}	N_{12}	$\bar{N}_{12}$	$\frac{N_{12}-\bar{N}_{12}}{N_{12}+\bar{N}_{12}}$	D_{OST}	D_{SST}^{meas}	D_{12}^{calc}	$\bar{D}_{12}^{calc}$	$\varepsilon \mathrm{D}^2(\mathrm{calc}), \%$
Min. p_t^{rel}	21944±199	277±19	2089±53	1483±50	1477±49	0.002±0.024	44.3 ± 2.2	0.5±5.3	44.7±4.8	43.9±4.8	0.343±0.525
Max. p_L^{rel}	21944±199	277±19	2089±53	1559±51	1390±48	0.057±0.024	44.3 ± 2.2	12.9±5.4	54.1±4.3	33.3±5.4	2.655±1.465
Max. p_t	21944±199	277±19	2089±53	1538±51	1408±48	0.044±0.024	44.3 ± 2.2	10.0±5.4	52.0±4.4	35.9±5.3	1.904±1.240
Min. $\lvert\Delta\vec{P}\rvert$	21944±199	277±19	2089±53	1573±51	1376±48	0.067±0.024	44.3 ± 2.2	15.1±5.4	55.7±4.3	31.3±5.6	3.272±1.629
Min. ΔR	21944±199	277±19	2089±53	1551±51	1398±48	0.052±0.024	44.3 ± 2.2	11.7±5.4	53.2±4.4	34.4±5.4	2.331±1.372
Max. $\cos\alpha$	21944±199	277±19	2089±53	1583±51	1371±48	0.072±0.024	44.3 ± 2.2	16.2±5.4	56.4±4.2	30.3±5.6	3.622±1.712
Min. $\cos\theta^*$	21944±199	277±19	2089±53	1568±51	1382±48	0.063±0.024	44.3 ± 2.2	14.2±5.4	55.1±4.3	32.1±5.5	3.021±1.564
Max. $\cos\theta^*$	21944±199	277±19	2089±53	1487±50	1475±49	0.004±0.024	44.3 ± 2.2	0.9±5.3	45.0±4.8	43.6±4.9	0.390±0.559
Min. $m(B_sK)$	21944±199	277±19	2089±53	1521±51	1442±49	0.027±0.024	44.3 ± 2.2	6.0±5.4	49.0±4.6	39.3±5.1	1.106±0.949
Aver. Q	15414±164	1110±43	8638±124	1095±42	1027±40	0.032±0.027	44.3 ± 2.2	7.2±6.2	49.9±5.1	38.3±5.8	1.275±0.952
$Q_{jet}(p_t, \kappa = 0.7)$	15629±165	1120±42	8419±124	1119±42	987±39	0.063±0.027	44.3 ± 2.2	14.1±6.2	55.0±4.8	32.2±6.2	2.577±1.359
"Comb. SST"	21941±199	277±19	2092±53	1477±50	1482±49	-0.002±0.024	44.3 ± 2.2	-0.4±5.3	44.0±4.8	44.6±4.8	0.265±0.462

Table 6: D_{SST} measured in data and corresponding ϵD^2

Tagger	N_{RT}	N_{WT}	N_{NT}	$\varepsilon, \%$	D, %	$\varepsilon \mathrm{D}^2, \%$
Min. p_t^{rel}	1254 ± 35	1064 ± 33	327 ± 18	87.6 ± 0.6	8.2 ± 2.1	0.589 ± 0.275
Max. p_L^{rel}	1232 ± 35	1086 ± 33	327 ± 18	87.6 ± 0.6	6.3 ± 2.1	0.348 ± 0.216
Max. p_t	1236 ± 35	1082 ± 33	327 ± 18	87.6 ± 0.6	6.6 ± 2.1	0.387 ± 0.227
Min. $\lvert\Delta\vec{P}\rvert$	1231 ± 35	1087 ± 33	327 ± 18	87.6 ± 0.6	6.2 ± 2.1	0.338 ± 0.213
Min. ΔR	1248 ± 35	1070 ± 33	327 ± 18	87.6 ± 0.6	7.7 ± 2.1	0.517 ± 0.259
Max. $\cos\alpha$	1245 ± 35	1073 ± 33	327 ± 18	87.6 ± 0.6	7.4 ± 2.1	0.483 ± 0.251
Min. $\cos\theta^*$	1233 ± 35	1085 ± 33	327 ± 18	87.6 ± 0.6	6.4 ± 2.1	0.357 ± 0.219
Max. $\cos\theta^*$	1189 ± 34	1129 ± 34	327 ± 18	87.6 ± 0.6	2.6 ± 2.1	0.059 ± 0.092
Min. $m(B_sK)$	1236 ± 35	1082 ± 33	327 ± 18	87.6 ± 0.6	6.6 ± 2.1	0.387 ± 0.227
Random track	1201 ± 35	1117 ± 33	327 ± 18	87.6 ± 0.6	3.6 ± 2.1	0.115 ± 0.127

Table 7: Comparison of different one-track taggers

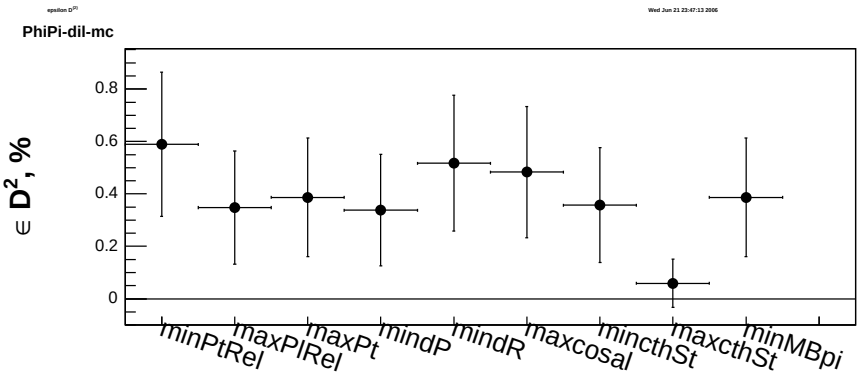

Figure 16: Comparison between $\varepsilon \mathrm{D}^2$'s for one-track taggers

A p14 Monte Carlo

For the comparison with the main course analysis p17 Monte Carlo we want to give dilutions and ϵD^2's obtained with p14 Monte Carlo in this Appendix. They are given in Table 7 and Figure 16 for one-track taggers, Table 8 and Figure 17 for two-track taggers, and Tables 9, 10, 11 and in Figure 18 for many-track taggers.

B Double Tagging with Uncorrelated Taggers

Suppose that we have two uncorrelated taggers with mistag rates p_1 and p_2 and that we apply them to a sample of N events. This sample can be separated into four subsamples:

- N_1 events tagged only by first tagger with dilution $D_1 = 1 - 2p_1$
- N_2 events tagged only by second tagger with dilution $D_2 = 1 - 2p_2$
- N_{12} events tagged by both taggers identically with *true* dilution D_{12}
- $\bar{N}_{12}$ events tagged by both taggers differently with *true* dilution $\bar{\mathrm{D}}_{12}$

Tagger	N_{RT}	N_{WT}	N_{NT}	$\varepsilon, \%$	D, %	$\varepsilon \mathrm{D}^2, \%$
$K^{*0} \to K\pi$	365 ± 19	326 ± 18	1954 ± 44	26.1 ± 0.9	5.6 ± 3.8	0.083 ± 0.108
$K^{*0} \to K\pi$(opt)	28 ± 5	22 ± 5	2595 ± 51	1.9 ± 0.3	12.0 ± 14.0	0.027 ± 0.060
Λ	7 ± 3	5 ± 2	2633 ± 51	0.5 ± 0.1	16.7 ± 28.5	0.013 ± 0.040

Table 8: Comparison of different two-track taggers

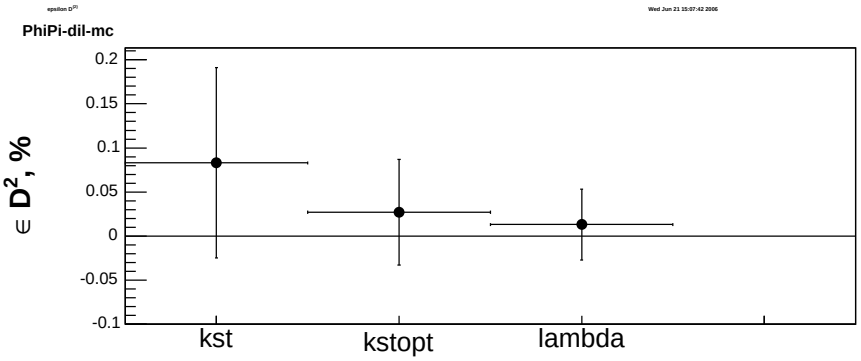

Figure 17: Comparison between $\varepsilon \mathrm{D}^2$'s for two-track taggers

Tagger	N_{RT}	N_{WT}	N_{NT}	$\varepsilon, \%$	D, %	$\varepsilon \mathrm{D}^2, \%$
Aver. Q	928 ± 30	778 ± 28	939 ± 31	64.5 ± 0.9	8.8 ± 2.4	0.499 ± 0.255
$Q_{jet}(p_t, \kappa = 0.1)$	893 ± 30	722 ± 27	1030 ± 32	61.1 ± 0.9	10.6 ± 2.5	0.685 ± 0.294
$Q_{jet}(p_t, \kappa = 0.2)$	889 ± 30	717 ± 27	1039 ± 32	60.7 ± 0.9	10.7 ± 2.5	0.696 ± 0.297
$Q_{jet}(p_t, \kappa = 0.3)$	892 ± 30	714 ± 27	1039 ± 32	60.7 ± 0.9	11.1 ± 2.5	0.746 ± 0.306
$Q_{jet}(p_t, \kappa = 0.4)$	910 ± 30	724 ± 27	1011 ± 32	61.8 ± 0.9	11.4 ± 2.5	0.800 ± 0.316
$Q_{jet}(p_t, \kappa = 0.5)$	927 ± 30	737 ± 27	981 ± 31	62.9 ± 0.9	11.4 ± 2.4	0.820 ± 0.320
$Q_{jet}(p_t, \kappa = 0.6)$	928 ± 30	756 ± 27	961 ± 31	63.7 ± 0.9	10.2 ± 2.4	0.664 ± 0.291
$Q_{jet}(p_t, \kappa = 0.7)$	939 ± 31	768 ± 28	938 ± 31	64.5 ± 0.9	10.0 ± 2.4	0.648 ± 0.287
$Q_{jet}(p_t, \kappa = 0.8)$	958 ± 31	784 ± 28	903 ± 30	65.9 ± 0.9	10.0 ± 2.4	0.657 ± 0.289
$Q_{jet}(p_t, \kappa = 0.9)$	966 ± 31	805 ± 28	874 ± 30	67.0 ± 0.9	9.1 ± 2.4	0.553 ± 0.267
$Q_{jet}(p_t, \kappa = 1.0)$	985 ± 31	814 ± 29	846 ± 29	68.0 ± 0.9	9.5 ± 2.3	0.615 ± 0.281

Table 9: Comparison of different charge-average taggers for p14 MC

Tagger	N_{RT}	N_{WT}	N_{NT}	$\varepsilon, \%$	D, %	$\varepsilon \mathrm{D}^2, \%$
Aver. Q	928 ± 30	778 ± 28	939 ± 31	64.5 ± 0.9	8.8 ± 2.4	0.499 ± 0.255
$Q_{jet}(p_t^{rel}, \kappa = 0.1)$	892 ± 30	729 ± 27	1024 ± 32	61.3 ± 0.9	10.1 ± 2.5	0.620 ± 0.281
$Q_{jet}(p_t^{rel}, \kappa = 0.2)$	882 ± 30	731 ± 27	1032 ± 32	61.0 ± 0.9	9.4 ± 2.5	0.534 ± 0.263
$Q_{jet}(p_t^{rel}, \kappa = 0.3)$	893 ± 30	746 ± 27	1006 ± 32	62.0 ± 0.9	9.0 ± 2.5	0.498 ± 0.255
$Q_{jet}(p_t^{rel}, \kappa = 0.4)$	910 ± 30	769 ± 28	966 ± 31	63.5 ± 0.9	8.4 ± 2.4	0.448 ± 0.242
$Q_{jet}(p_t^{rel}, \kappa = 0.5)$	914 ± 30	787 ± 28	944 ± 31	64.3 ± 0.9	7.5 ± 2.4	0.358 ± 0.219
$Q_{jet}(p_t^{rel}, \kappa = 0.6)$	931 ± 31	809 ± 28	905 ± 30	65.8 ± 0.9	7.0 ± 2.4	0.323 ± 0.208
$Q_{jet}(p_t^{rel}, \kappa = 0.7)$	944 ± 31	827 ± 29	874 ± 30	67.0 ± 0.9	6.6 ± 2.4	0.292 ± 0.199
$Q_{jet}(p_t^{rel}, \kappa = 0.8)$	968 ± 31	844 ± 29	833 ± 29	68.5 ± 0.9	6.8 ± 2.3	0.321 ± 0.208
$Q_{jet}(p_t^{rel}, \kappa = 0.9)$	987 ± 31	858 ± 29	800 ± 28	69.8 ± 0.9	7.0 ± 2.3	0.341 ± 0.214
$Q_{jet}(p_t^{rel}, \kappa = 1.0)$	1002 ± 32	873 ± 30	770 ± 28	70.9 ± 0.9	6.9 ± 2.3	0.336 ± 0.212

Table 10: Comparison of different charge-average taggers for p14 MC

Tagger	N_{RT}	N_{WT}	N_{NT}	$\varepsilon, \%$	D, %	$\varepsilon \mathrm{D}^2, \%$
Aver. Q	928 ± 30	778 ± 28	939 ± 31	64.5 ± 0.9	8.8 ± 2.4	0.499 ± 0.255
$Q_{jet}(p_L^{rel}, \kappa = 0.1)$	890 ± 30	720 ± 27	1035 ± 32	60.9 ± 0.9	10.6 ± 2.5	0.679 ± 0.293
$Q_{jet}(p_L^{rel}, \kappa = 0.2)$	891 ± 30	712 ± 27	1042 ± 32	60.6 ± 1.0	11.2 ± 2.5	0.756 ± 0.308
$Q_{jet}(p_L^{rel}, \kappa = 0.3)$	899 ± 30	709 ± 27	1037 ± 32	60.8 ± 0.9	11.8 ± 2.5	0.849 ± 0.324
$Q_{jet}(p_L^{rel}, \kappa = 0.4)$	901 ± 30	719 ± 27	1025 ± 32	61.2 ± 0.9	11.2 ± 2.5	0.773 ± 0.311
$Q_{jet}(p_L^{rel}, \kappa = 0.5)$	930 ± 30	742 ± 27	973 ± 31	63.2 ± 0.9	11.2 ± 2.4	0.799 ± 0.316
$Q_{jet}(p_L^{rel}, \kappa = 0.6)$	940 ± 31	766 ± 28	939 ± 31	64.5 ± 0.9	10.2 ± 2.4	0.671 ± 0.292
$Q_{jet}(p_L^{rel}, \kappa = 0.7)$	947 ± 31	782 ± 28	916 ± 30	65.4 ± 0.9	9.5 ± 2.4	0.595 ± 0.276
$Q_{jet}(p_L^{rel}, \kappa = 0.8)$	961 ± 31	800 ± 28	884 ± 30	66.6 ± 0.9	9.1 ± 2.4	0.557 ± 0.268
$Q_{jet}(p_L^{rel}, \kappa = 0.9)$	978 ± 31	818 ± 29	849 ± 29	67.9 ± 0.9	8.9 ± 2.4	0.539 ± 0.264
$Q_{jet}(p_L^{rel}, \kappa = 1.0)$	1000 ± 32	837 ± 29	808 ± 28	69.5 ± 0.9	8.9 ± 2.3	0.547 ± 0.266

Table 11: Comparison of different charge-average taggers for p14 MC

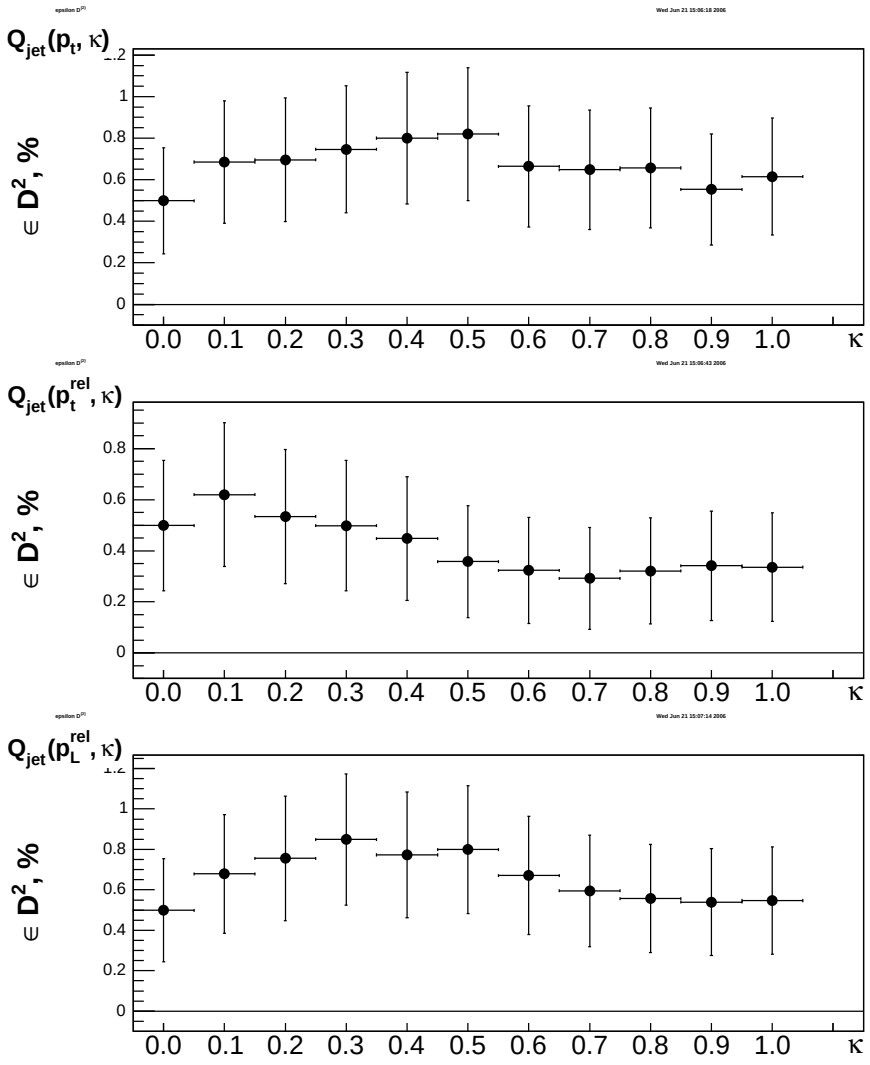

Figure 18: Comparison between εD^2's for charge-average taggers for p14 MC

Let us consider the third group of events. The probability for the event to fall into this group is equal to $p_1p_2+(1-p_1)(1-p_2)$. The mistag rate for this group, then, equals $p_{12} = \frac{p_1p_2}{p_1p_2+(1-p_1)(1-p_2)}$ and the dilution is $D_{12} = 1-2p_{12} = \frac{(1-p_1)(1-p_2)-p_1p_2}{(1-p_1)(1-p_2)+p_1p_2}$. This expression can be rewritten as

$$D_{12} = \frac{1-2p_1+1-2p_2}{1+(1-2p_1)(1-2p_2)} = \frac{D_1+D_2}{1+D_1D_2}. \quad (1)$$

Similarly, for the fourth group,

$$\bar{D}_{12} = \frac{|D_1-D_2|}{1-D_1D_2}. \quad (2)$$

This derivation for the case of more than two taggers can be found in Reference [4].

If the event is tagged with both taggers, then the probability to obtain the identical results ("Same Sign") from them is

$$p_{SS} = N_{12}/(N_{12}+\bar{N}_{12}).$$

Similarly, for opposite tagging results ("Opposite Sign"):

$$p_{OS} = \bar{N}_{12}/(N_{12}+\bar{N}_{12}).$$

These probabilities can be easily expressed in terms of the probabilities p_1 and p_2:

$$p_{SS} = p_1p_2+(1-p_1)(1-p_2), p_{OS} = p_1(1-p_2)+(1-p_1)p_2.$$

From these formulas it follows that

$$p_{SS}-p_{OS} = \frac{N_{12}-\bar{N}_{12}}{N_{12}+\bar{N}_{12}} = (1-2p_1)(1-2p_2) = D_1\cdot D_2$$

i.e. the dilution of one of the taggers, D_1, can be measured in the data if the second dilution, D_2, is known:

$$D_1 = \frac{1}{D_2}\cdot\frac{N_{12}-\bar{N}_{12}}{N_{12}+\bar{N}_{12}}. \quad (3)$$

Then the other two dilutions, D_{12} and $\bar{D}_{12}$, can be calculated according to Eqns. 1 and 2. Of course, these formulae are only apply in case of uncorrelated taggers. The "ϵD^2" can be obtained as follows:

$$\epsilon D^2 = \frac{N_{tag}}{N}\cdot\left(\frac{N_1}{N_{tag}}\cdot D_1+\frac{N_2}{N_{tag}}\cdot D_2+\frac{N_{12}}{N_{tag}}\cdot D_{12}+\frac{\bar{N}_{12}}{N_{tag}}\cdot\bar{D}_{12}\right)^2, \quad (4)$$

where $N_{tag} = N_1+N_2+N_{12}+\bar{N}_{12}$ is the number of tagged events.